

Research Article

Thermodynamic Analysis of Evaporation of Levitated Binary and Ternary Liquid Fuel Droplets under Normal Gravity

S. Raghuram and Vasudevan Raghavan

Department of Mechanical Engineering, Indian Institute of Technology Madras, Chennai, Tamilnadu 600036, India

Correspondence should be addressed to Vasudevan Raghavan, raghavan@iitm.ac.in

Received 31 March 2012; Accepted 18 May 2012

Academic Editors: H. Binder, S. Hashimoto, R. D. Simitev, and P. Trens

Copyright © 2012 S. Raghuram and V. Raghavan. This is an open access article distributed under the Creative Commons Attribution License, which permits unrestricted use, distribution, and reproduction in any medium, provided the original work is properly cited.

The present study presents a thermodynamic model for predicting the vaporization characteristics of binary and ternary hydrocarbon fuel droplets under atmospheric pressure and normal gravity conditions. The model employs activity coefficients based on UNIFAC group contribution method and evaluates the vapor-liquid equilibrium of binary and ternary droplets. The gas-phase properties have been evaluated as a function of temperature and mixture molecular weight. The model has been validated against the experimental data available in literature. The validated model is used to predict the vaporization characteristics of binary and ternary fuel droplets at atmospheric pressure under normal gravity. Results show multiple slopes in the droplet surface regression indicating preferential vaporization of fuel components based on their boiling point and volatility. The average evaporation rate is dictated by the ambient temperature and also by composition of the mixture.

1. Introduction

The process of evaporation of atomized fuel droplets in a combustion chamber plays an important role in achieving high efficiency and in reducing emissions in liquid fuel combustion systems such as gas turbines and industrial boilers. Due to increasing demand of fossil fuels, alternative biofuels are being tested in several applications. To avoid major modifications in the system or engine, these biofuels are blended with fossil fuels. Further, these fuels are multicomponent in nature; comprised of a blend of several compounds having different physical, chemical, and thermal properties. To characterize these fuel blends and to obtain chemical kinetics data for these fuel types, surrogates are employed. Surrogates are blend of pure fuels such as liquid hydrocarbon fuels. This may be, for instance, n-heptane, n-octane, and n-hexadecane mixed in different proportions. When such blended fuel droplets, having constituents with different volatilities, vaporize, the trend will be much different than that of a pure single-component fuel droplet. Study of evaporation behavior of a multicomponent droplet is therefore complex and needs attention.

Several studies on multicomponent fuel droplets are available. Tong and Sirignano [1] developed a simplified model for multicomponent fuel droplet vaporization in a hot convective environment. Their model, however, over predicted the experimental results under convective situations. Tamim and Hallett [2] used a continuous thermodynamics model to describe the mixture composition, properties, and vapor-liquid equilibrium. In their model, the composition was represented by a continuous probability density function (pdf). Their model required construction of distribution function based on the knowledge of fuel mixture composition obtained from experiments. Yang et al. [3] used a discrete/continuous multicomponent model (DCMC) to describe the composition of realistic fuels. Gasoline is assumed to consist of five discrete families of hydrocarbons, each consisting of infinite number of continuous components, modeled as pdfs. They claimed that their procedure gave more accurate predictions when compared to a continuous model.

Aggarwal and Mongia [4] used surrogate fuel droplet to represent vaporization behavior of a multicomponent droplet. Different models such as diffusion-limit and

TABLE 1: Properties of the hydrocarbon fuels such as molecular weight, M , liquid-phase density, ρ_l , normal boiling point, T_b , latent heat of vaporization, h_{fg} , Lennard-Jones potential, σ , and ϵ/k .

Hydrocarbon fuel	Physical properties					
	M (kg/kmol)	ρ_l (kg/m ³)	T_b (K)	h_{fg} (J/kg)	σ (Å)	ϵ/k (K)
n-Heptane	100	684	371.6	316700	6.116	429.05
n-Octane	114	703	398.8	302000	6.387	451.68
n-Nonane	128	718	424	293800	6.620	472.17
n-Decane	142	730	447.3	281000	6.835	490.51
n-Dodecane	170	748	489.5	255300	7.227	522.67
n-Hexadecane	226	773	560	232000	8.181	573.33

infinite-diffusion models were used by them to compare the behavior of multicomponent fuel with that of the surrogate fuel. They investigated the operating conditions under which their assumptions were valid. Convective evaporation of decane-hexadecane binary hydrocarbon droplet at high temperatures was studied by Renksizbulut and Bussmann [5]. They showed that existing Nusselt number correlations used for single-component droplets can be used for multicomponent droplets as well. They have, however, not examined its validity for wide range of temperatures. A model for unsteady droplet vaporization for a wide range of temperatures was developed by Ra and Reitz [6]. An unsteady internal heat flux model and a model to determine droplet surface temperature were proposed in their work. They have simulated single-component droplet evaporation. Gartung et al. [7] investigated two different droplet vaporization models, discrete and continuous models, to describe multicomponent vaporization of hydrocarbon blends. Chen et al. [8] investigated the vaporization of both single-component and multicomponent fuel droplets injected into a hot-laminar flow using three different liquid-phase models: infinite-diffusion, diffusion-limit, and thin-skin models. They found that their predictions were in agreement with experimental data. Wilms [9] carried out his thesis work on laser-based levitation of hydrocarbon fuel droplets and their blends and reported experimental data for low pressure, and low temperature evaporation characteristics.

This paper presents a simplified thermodynamic model to simulate multicomponent droplet vaporization under atmospheric pressure and normal gravity. This model is based on infinite-diffusivity assumption for the liquid phase and uses UNIFAC group contribution method to evaluate the activity coefficients required for calculating vapor-liquid equilibrium. The gas-phase properties such as density and mass diffusivity have been evaluated as functions of temperature and molecular weight. The results obtained from the numerical model have been validated against the experimental data reported in Wilms (2005) [9]. The validated model is used to carry out parametric studies at atmospheric pressure under normal gravity, for a range of ambient temperatures (350 K–500 K). The parameters of interest such as the time histories of droplet surface area, liquid-phase composition, surface temperature, and

the evaporation constant have been predicted. The droplet lifetime variation as a function of fuel composition and ambient temperature is also studied.

2. Thermodynamic Model

The mathematical model is based on the following assumptions: (1) the droplet is spherical throughout its lifetime; (2) mass diffusion in both liquid and vapor phase obey Fick's law of diffusion; (3) diffusivity of the liquid phase is infinitely high, due to rapid mixing and hence the temperature distribution within the droplet is assumed to be uniform, therefore, spatial variations of properties are neglected and only temporal variations are considered; (4) the liquid and the vapor phases are in thermodynamic equilibrium with each other; (5) ambient air is insoluble in the liquid phase; (6) Lewis number at the interface is unity; (7) radiative heat transfer is neglected; (8) Soret and Dufour effects are neglected

The evaporation rate, dm/dt (kg/s), is calculated every time step using Nusselt number, Nu , the vapor-phase density of the mixture, ρ (kg/m³), instantaneous droplet diameter, d (m), the mass transfer number, B_M , and the mass diffusivity of the fuel to air in vapor phase, D_{f-air} (m²/s), as given below [10]

$$\frac{dm}{dt} = \pi d \rho D_{f-air} Nu [\ln(1 + B_M)]. \quad (1)$$

The binary mass diffusivity of a fuel component diffusing into air, at the reference temperature of 300 K, is calculated using correlation that utilizes Lennard-Jones potential [10]. Table 1 provides the Lennard-Jones potential used in the calculations for several fuels (n-pentane, n-hexane, n-heptane, n-octane, n-nonane, n-decane, n-dodecane, n-hexadecane). A curve fit is obtained for the mass diffusivity as a function of molecular mass of the fuel. The mass diffusivity of a fuel mixture diffusing into air is then calculated using that curve fit, where instead of pure component molecular mass, the molecular mass of the fuel mixture ($M_{f,mix}$) would be used as follows:

$$D_{f-air}(300\text{ K}) = 12.49 \times 10^{-5} (M_f)^{-0.57}. \quad (2)$$

Diffusivity at the required temperature is then calculated using the following equation [11]:

$$D_{f\text{-air}}(T) = \left(\frac{T}{300}\right)^{1.75} D_{f\text{-air}}(300). \quad (3)$$

The mass transfer number, B_M , used in (1) is given by [10]:

$$B_M = \frac{Y_{fs}}{1 - Y_{fs}}, \quad (4)$$

where Y_{fs} is the mass fraction of the fuel mixture at the droplet surface, obtained as

$$Y_{fs} = \sum_i Y_i = 1 - Y_{\text{air}}, \quad (5)$$

where Y_i is the vapor-phase mass fraction of each fuel species i and Y_{air} is the vapor-phase mass fraction of air. From this, total mass lost from the liquid phase (Δm) due to evaporation during the time interval, Δt , is calculated as given below

$$\Delta m = \frac{dm}{dt} \Delta t. \quad (6)$$

For calculating the individual species mass evaporated during the time interval Δt , scaled mass fractions ($Y_{i,s}$) of individual fuel in the vapor phase are calculated such that air is excluded and when added they sum to unity. Then the individual fuel mass evaporated will be given as follows:

$$\Delta m_i = Y_{i,s} \Delta m. \quad (7)$$

The evaporated mass of individual fuel species is subtracted from the respective masses available during the start of the time interval, and the mass and mole fractions of each species in the liquid phase are recalculated based on the new mass. The new diameter of the droplet for the new time step is obtained from the new liquid phase mass, based on the assumption that the droplet is spherical and homogeneous mixture prevails in liquid phase (infinite diffusion assumption).

The Nusselt number used in (1) is calculated from the Ranz-Marshall correlation (as the Reynolds numbers involved in the analysis are small), by setting $\text{Pr} = 1$ [11] as follows

$$\text{Nu} = 2 + 0.6 \text{Re}_{\text{eff}}^{0.5}, \quad \text{Re}_{\text{eff}} < 2000, \quad (8)$$

where Re_{eff} is the effective Reynolds number for mixed convection, calculated using Reynolds number (Re) for forced convection and Grashoff number (Gr) and is given by

$$\text{Re}_{\text{eff}} = \text{Re} + \text{Gr}^{0.5}. \quad (9)$$

The Reynolds and Grashoff numbers are calculated using as the velocity of the air flow, V (m/s), the instantaneous droplet diameter, d (m), and the kinematic viscosity of the vapor-phase, ν (m^2/s), as follows:

$$\text{Re} = \frac{Vd}{\nu}, \quad \text{Gr} = \frac{g\beta\Delta T d^3}{\nu^2}. \quad (10)$$

In (10), g is acceleration due to gravity, ΔT is the difference between the ambient (T_∞) and the surface temperature (T_s), and β is the coefficient of thermal expansion [$2/(T_\infty + T_s)$]. The surface temperature of the droplet is evaluated by an iterative process, such that equilibrium prevails between the vapor and liquid phases. At equilibrium, when all of the heat transferred to the drop is used to vaporize the fuel, the following condition is used:

$$B_T = B_M, \quad (11)$$

where B_T is the transfer number for heat transfer, given as [10]

$$B_T = \frac{C_p(T_\infty - T_s)}{h_{fg,f}}, \quad (12)$$

where C_p is the specific heat of the gas mixture at the interface (J/kg-K), calculated at the average temperature, and $h_{fg,f}$ is the latent heat of vaporization of the fuel mixture (J/kg), calculated using scaled mass fractions and mixing law as follows:

$$h_{fg,f} = \sum_i Y_{i,s} h_{fg,i}. \quad (13)$$

In order to calculate the mass fractions of the fuel components, the vapor-phase mole fractions of the fuel species are obtained from vapor-liquid equilibrium, given as

$$y_i P = x_i \gamma_i P_{vp,i}, \quad (14)$$

where y_i is the vapor-phase mole fraction of fuel species i , x_i is the liquid-phase mole fraction of fuel species i , P is the total pressure (Pa), $P_{vp,i}$ is the vapor pressure of fuel species i (Pa) evaluated using the Wagner equation [12], and γ_i is the activity coefficient of fuel species i , evaluated using the UNIFAC group contribution method [12, 13]. The mole fraction of air at the interface is calculated by the material balance equation, given as

$$y_{\text{air}} = 1 - \sum_i y_i, \quad (15)$$

where y_{air} is the vapor-phase mole fraction of air at the interface.

The above equations are solved until the droplet diameter reduces to zero. The liquid-phase composition and the equilibrium surface temperature are updated for each time step.

3. Results and Discussion

First, the thermodynamic model is validated against the experimental results from Wilms [9]. Wilms [9] has performed experiments with suspended droplets levitated optically using various pure component as well as binary and ternary mixtures of hydrocarbon fuels. In their experimental setup, the droplets are injected into a heated chamber using a droplet-on-demand generator and the droplet size is measured using the rainbow refractometry, morphology

dependent resonances, or Mie scattering imaging [9]. A gentle flow of air, in the range of 0.1–1 cm/s, has been supplied to evacuate the vapors from the heated chamber [9].

A few cases of levitated vaporization of binary and ternary mixtures of hydrocarbon fuels have been simulated using present model in order to compare the numerical results against the experimental results reported in Wilms [9]. For the validation cases, apart from the buoyancy induced flow due to the presence of normal gravity, a forced convective flow with a velocity of 1 cm/s is also considered. Therefore, in these cases the effective Reynolds number has contributions from both forced convective Reynolds number as well as the Grashoff number.

Figure 1 shows the comparison of the theoretical surface regression results for binary and ternary fuel droplets, with the experimental data reported in Wilms [9]. In all the cases, the initial droplet diameter has been taken as 50 μm , and the ambient pressure is taken as atmospheric pressure. For the case of binary droplet mixture, an initial blend having 73% by volume of n-heptane ($Z_{01} = 0.73$) and 27% by volume of n-hexadecane ($Z_{02} = 0.27$) is chosen, where Z_{0i} denotes the initial volume fraction of fuel component i in the mixture. The ambient temperature for this case has been chosen as 299.4 K. For ternary droplets, three different blends have been considered: (1) equal volumes of n-octane, n-nonane, and n-decane ($T_{\infty} = 299.9$ K), (2) equal volumes of n-octane, n-decane, and n-dodecane ($T_{\infty} = 299.2$ K), and (3) equal volumes of n-octane, n-dodecane, and n-hexadecane ($T_{\infty} = 296.5$ K). Figure 1 shows that the thermodynamic model is able to predict the surface regression history of all the cases quite close to the experimental measurements. This shows that the model can be used to study the parametric effect in binary and ternary droplet vaporization. For parametric studies, the compositions of the blends and the ambient temperatures have been varied. The initial droplet diameter and its temperature are kept as 50 μm and 300 K, respectively. Only natural convection under atmospheric pressure is considered for all cases. Table 1 presents the properties of the fuels used in the present study.

3.1. Effect of Mixture Composition. Figure 2 shows the time histories of surface regression for binary and ternary droplets having different initial compositions, evaporating at an ambient temperature of 450 K. In the case of binary droplets, n-heptane and n-hexadecane are considered in different volumetric proportions ($Z_{01} = 0.2, 0.4, 0.6, 0.8$). In the case of ternary droplets, n-octane, n-dodecane, and n-hexadecane are considered in different volumetric proportions, but with a fixed volume fraction of n-dodecane as 0.2, ($Z_{01} = 0.2, 0.4, 0.6$; $Z_{02} = 0.2$). The time histories of surface regression of pure components are also shown in dark solid lines for comparison.

Figure 2(a) clearly shows that n-heptane in the binary mixture preferentially vaporizes at a much faster rate when compared to that of n-hexadecane due to higher boiling point and lower volatility of the latter species. Therefore, the initial regression is coinciding with pure n-heptane line ($Z_{01} = 1$). Figure 3(a) presents the liquid-phase mole

fraction of n-heptane, for various initial volume fractions of n-heptane in the binary n-heptane-n-hexadecane mixture.

It can be noted that n-heptane evaporates almost completely, around 0.007 s, for the case where its initial volume fraction is equal to 0.2. From that instant, the regression line is parallel to that of n-hexadecane ($Z_{02} = 1$) as shown in Figure 2, that is, after the consumption of n-heptane, n-hexadecane starts to evaporate with a much smaller regression rate; the droplet lifetime increases with a decrease in the n-heptane fraction in the blend. In the case of ternary blends, preferential vaporization of n-octane takes place at a higher rate due to its lowest boiling point and higher volatility (Figure 2(b)). However, contrary to the sharp change in the slopes of the regression rates as observed in the case of binary mixtures, the slopes of the regression rates gradually change and become parallel to that of n-hexadecane, for the composition considered. This is because of the fact that towards the end of n-octane consumption, n-dodecane, and, to some extent, n-hexadecane start to vaporize, due to marginal increase in the equilibrium surface temperature.

Figure 4 shows the time histories of equilibrium surface temperature for both binary and ternary mixtures. For instance, considering the ternary mixture, $Z_{01} = 0.4$, $Z_{02} = 0.2$ and $Z_{03} = 0.4$, it is clear that n-octane is consumed around 0.0175 s (Figure 3(b)), and around that time the equilibrium surface temperature has reached around 400 K (Figure 4(b)).

Therefore, after that period, since the surface temperature is higher enough (around 400 K), both n-dodecane and n-hexadecane vaporize simultaneously; however, the rate of vaporization of n-hexadecane will be much lower than n-dodecane. This is noted by the nonlinearity in the regression curve (Figure 2(b)). Once all of the n-dodecane is vaporized, the regression curve becomes parallel to that of n-hexadecane line.

A notable change between the temporal variations of surface temperature between the binary and ternary mixtures is three-slope variation in the case of ternary (Figure 4). It can also be noted from Figure 4(a) that, in the case of binary mixture, once the first component fully vaporizes, the equilibrium temperature remains constant, well below the normal boiling point of the second component. In case of ternary mixtures, a gradual variation in surface temperature with time is observed (Figure 4(b)) and it reaches an almost constant value, same as in the case of binary mixture owing to the fact that the third component in ternary mixture is same as the second component in the case of binary mixture.

The temporal variation of the evaporation constant, K (m^2/s), is shown in Figure 5 for binary and ternary droplets. In the case of binary droplet, the evaporation constant value decreases much gradually as the most volatile (first) component vaporizes and suddenly decreases to a constant low value after the first fuel component fully vaporizes. The lower evaporation rate is the one at which the second component steadily vaporizes.

In the case of ternary mixtures, a threefold slope variation is observed in K versus time curve (Figure 5(b)). After the rapid decrease in the K value once the first component is

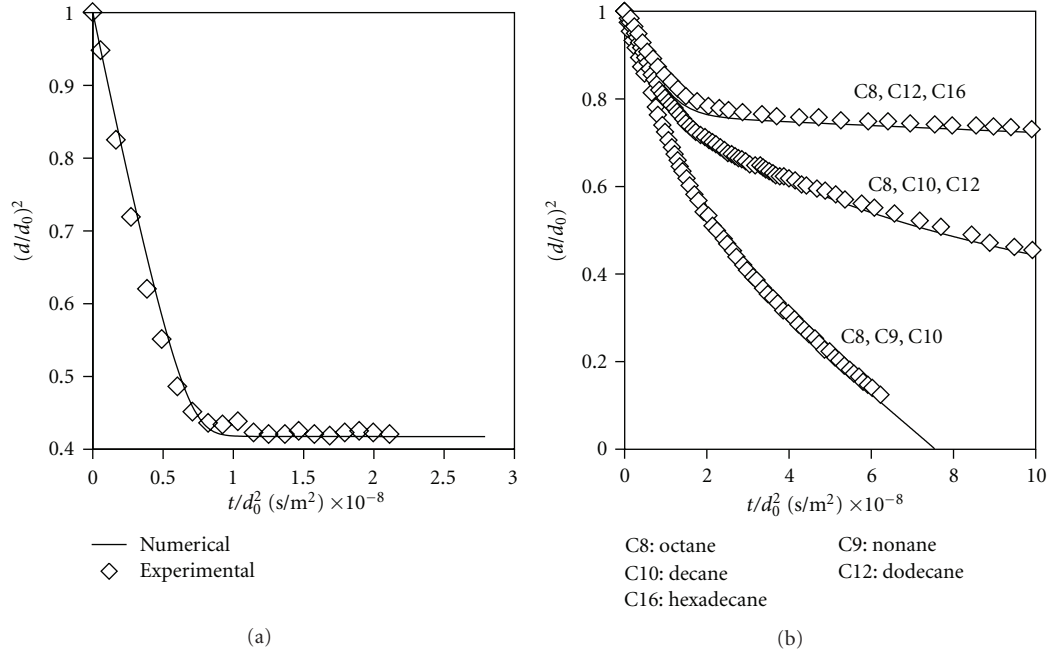


FIGURE 1: Time histories of droplet surface regression for: (a) binary mixture of n-heptane ($Z_{01} = 0.73$) and n-hexadecane ($Z_{02} = 0.27$) evaporating at an ambient temperature of 299.4 K, (b) different ternary mixtures containing equal volumes of three hydrocarbon fuels; n-octane, n-nonane, and n-decane ($T_\infty = 299.9$ K); n-octane, n-decane, and n-dodecane ($T_\infty = 299.2$ K); and n-octane, n-dodecane, n-hexadecane ($T_\infty = 296.5$ K).

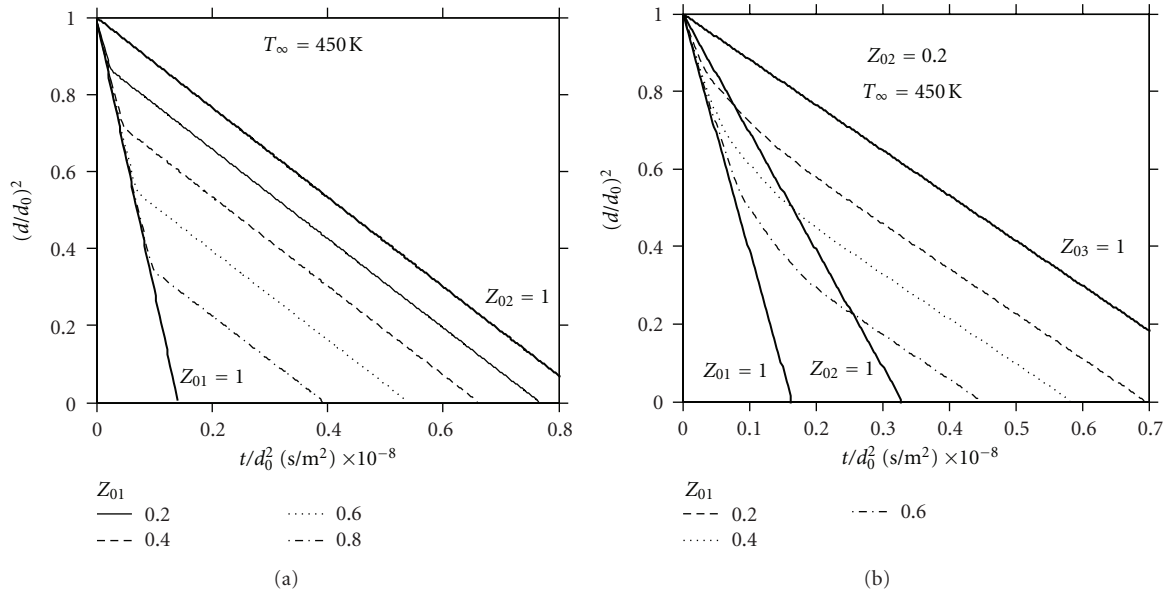


FIGURE 2: Time histories of surface regression of (a) binary (n-heptane and n-hexadecane) and (b) ternary (n-octane, n-dodecane, and n-hexadecane) mixtures of different initial compositions evaporating at an ambient temperature of 450 K.

consumed, K decreases much gradually to reach a constant minimum value. In this period, as discussed above, both n-dodecane and n-hexadecane vaporize simultaneously. Once n-dodecane is fully consumed, n-hexadecane evaporates at the lowest steady rate.

3.2. Effect of Ambient Temperature. Figure 6 shows the effect of varying ambient temperature on the time histories of droplet surface regression for binary and ternary mixtures having a fixed composition. A binary mixture of n-heptane, 40% by volume and n-hexadecane, 60% by volume, is

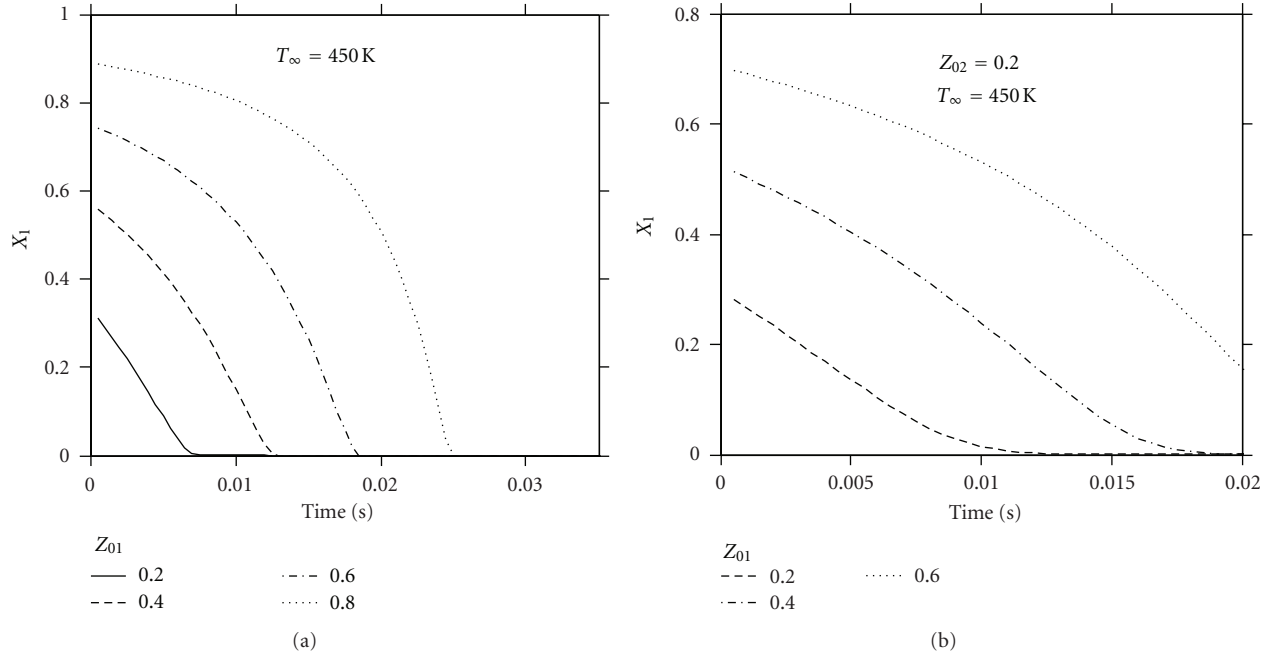


FIGURE 3: Temporal variation of liquid-phase mole fraction of the first fuel component for various initial compositions in (a) binary (n-heptane, and n-hexadecane) mixture, (b) ternary (n-octane, n-dodecane, and n-hexadecane) mixture evaporating at an ambient temperature of 450 K.

considered and a ternary mixture of n-octane, 40% by volume, n-dodecane, 20% by volume, and rest n-hexadecane is considered. It is clearly observed that the droplet lifetime decreases almost exponentially with increasing ambient temperature. This effect is more significant for the composition considered for the ternary mixture.

Figure 7 shows the variation of equilibrium droplet surface temperature with time for both binary and ternary droplets at different ambient temperatures. Equilibrium surface temperature increases with ambient temperature and forms the reason for reduction in the lifetime. The variation trend of surface temperature is as discussed with respect to Figure 4. Furthermore, in Figure 6, the distinct change in the slope of the surface regression curve signifies the completion of the vaporization of the most volatile component and also the time at which the most volatile component vaporizes completely, decreases with increasing ambient temperature.

Figure 8 shows the temporal variation of the evaporation constant for binary and ternary droplets with fixed composition and at different ambient temperatures. Clearly, the time at which the evaporation constant suffers a rapid decrease due to the consumption of the first component, decreases with increasing ambient temperature. Also, the lowest value of the evaporation constant, at which n-hexadecane vaporizes towards the end, is seen to increase with an increase in the ambient temperature.

Figure 9 shows the variation of time-averaged evaporation constant (K_{avg}) with ambient temperature for different initial compositions of binary mixture (n-heptane, and

n-hexadecane). It is observed that the average evaporation constant increases exponentially with ambient temperature for the range considered. Further, when the amount of n-heptane in the fuel mixture is higher, the average evaporation constant is also higher due to the faster vaporizing component (n-heptane) residing in the mixture for a longer time. As the ambient temperature increases, the overall ratio of the evaporation constants of blends having 80% n-heptane and 20% n-heptane decreases. The effect of ambient temperature rise is much higher than the effect of increase of n-heptane in the mixture. For the binary mixture, comprised of n-heptane and n-hexadecane, the time-averaged evaporation constant is seen to increase by around 225-times as the temperature is increased from 350 K to 500 K, for the composition having 80% n-heptane and 20% n-hexadecane and when the ambient temperature is kept at 350 K. When the n-heptane volume percentage is increased from 20% to 80%, around 2.5-times increase in average evaporation value is observed at the ambient temperature of 350 K.

Figure 10 shows the variation of time-averaged evaporation constant with ambient temperature for different initial compositions of ternary mixture (n-octane, n-dodecane, and n-hexadecane). The variation trends are similar to those of binary mixture. In the ternary case, the volume fraction of n-octane in the blend dictates the value of average evaporation constant apart from the ambient temperature. For a blend composition of 20% n-octane, 20% n-dodecane, and 80% n-hexadecane, when the ambient temperature is increased from 350 K to 500 K, around 195-times increase in the average evaporation constant is achieved.

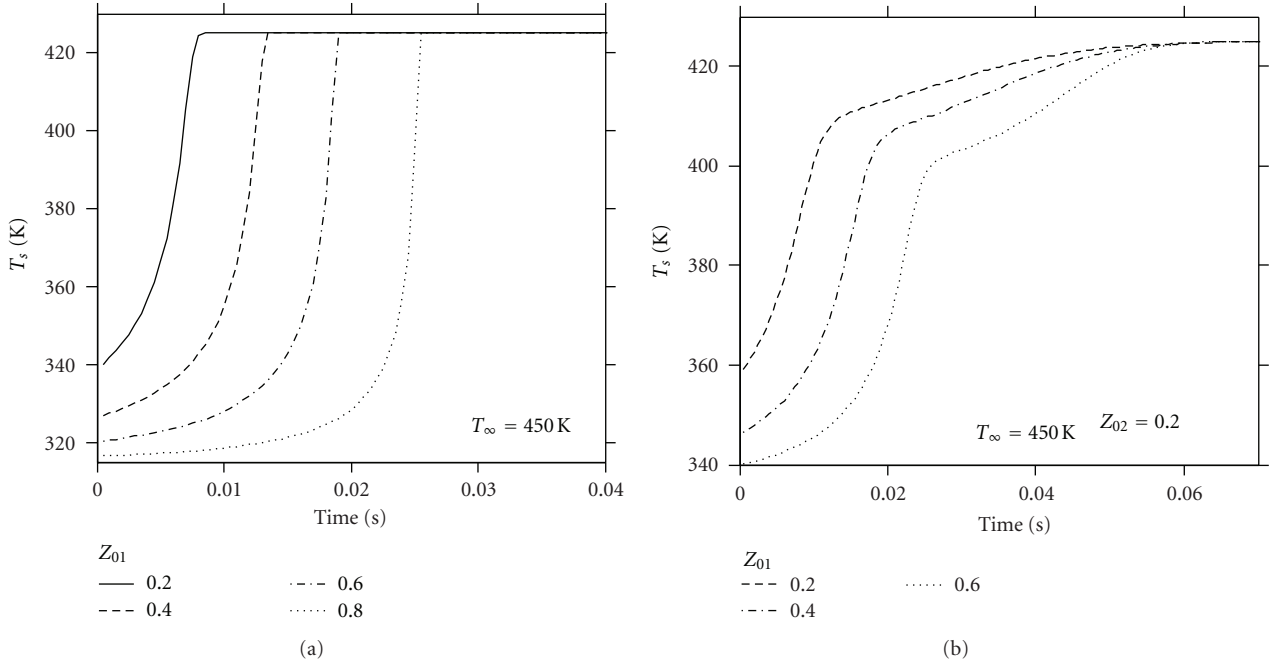


FIGURE 4: Temporal variation of equilibrium surface temperature during the evaporation of (a) binary mixture and (b) ternary mixture at an ambient temperature of 450 K.

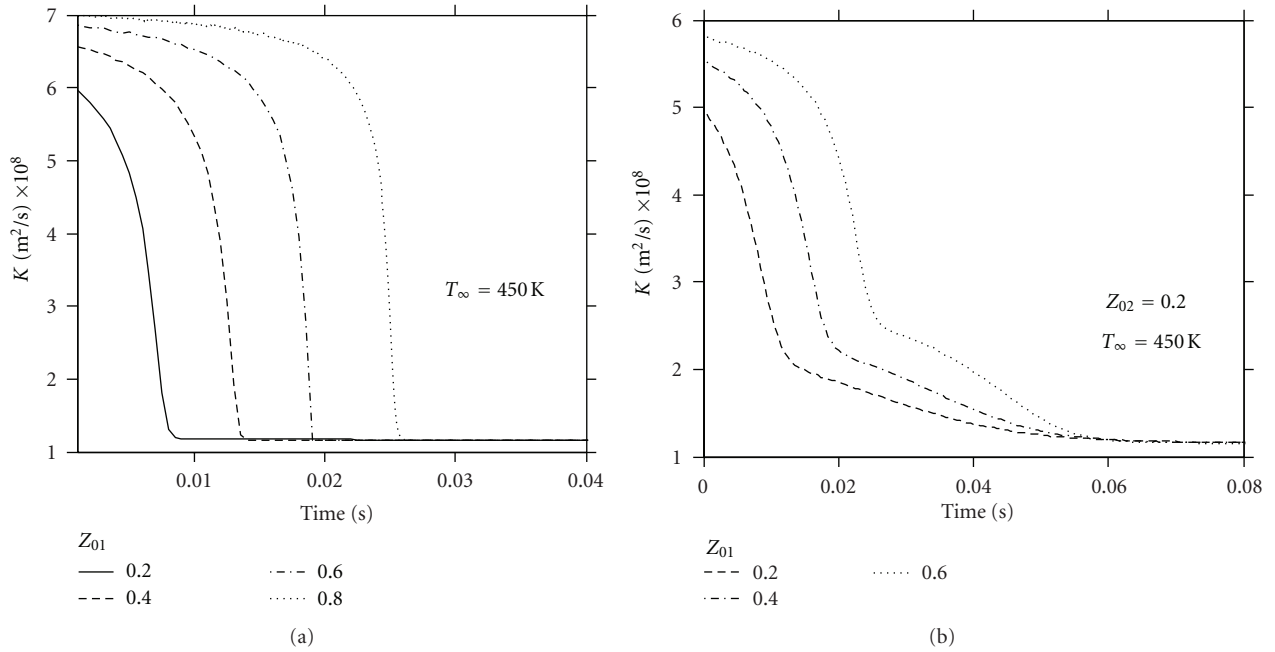


FIGURE 5: Temporal variation of the evaporation constant during the evaporation of (a) binary mixture and (b) ternary mixture at an ambient temperature of 450 K.

4. Conclusions

This paper presents a simplified thermodynamic model to simulate atmospheric pressure multicomponent droplet vaporization. This model is based on infinite-diffusivity assumption for the liquid phase and uses UNIFAC group

contribution method to evaluate the activity coefficients required for calculating vapor-liquid equilibrium. The gas-phase properties such as density and mass diffusivity have been evaluated as functions of temperature, and molecular weight. The results obtained from the thermodynamic model have been validated against the experimental data reported

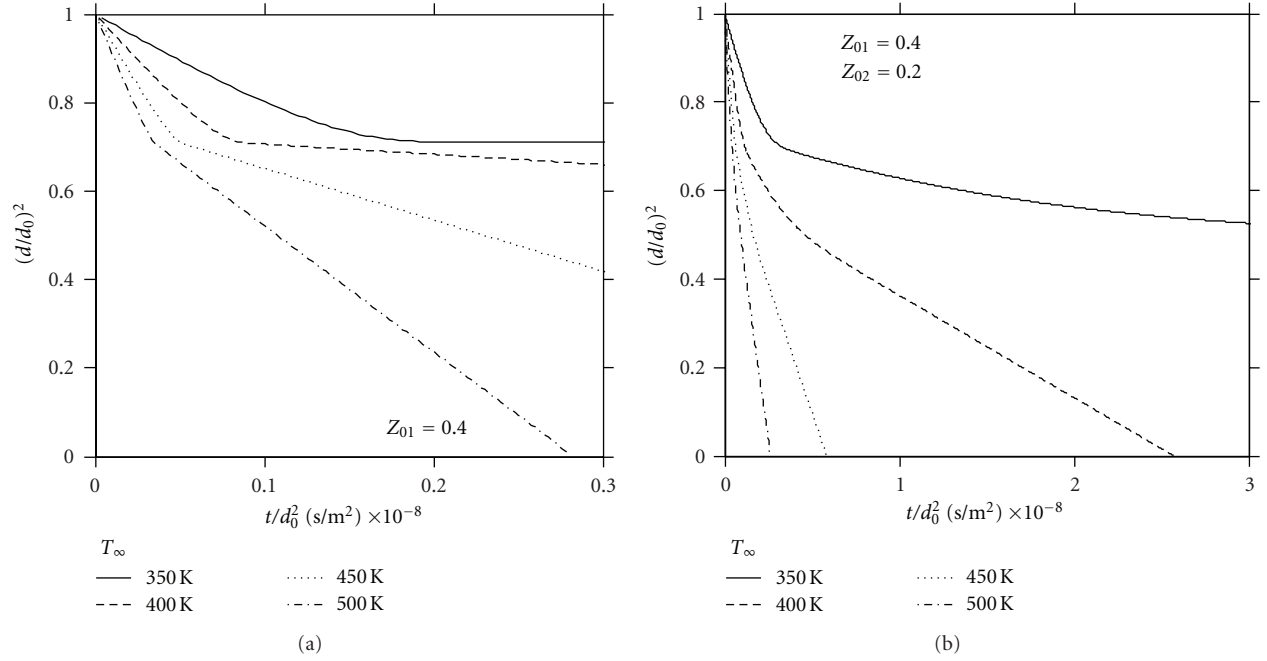


FIGURE 6: Time histories of droplet surface regression at various ambient temperatures for a given initial composition of (a) binary mixture and (b) ternary mixture.

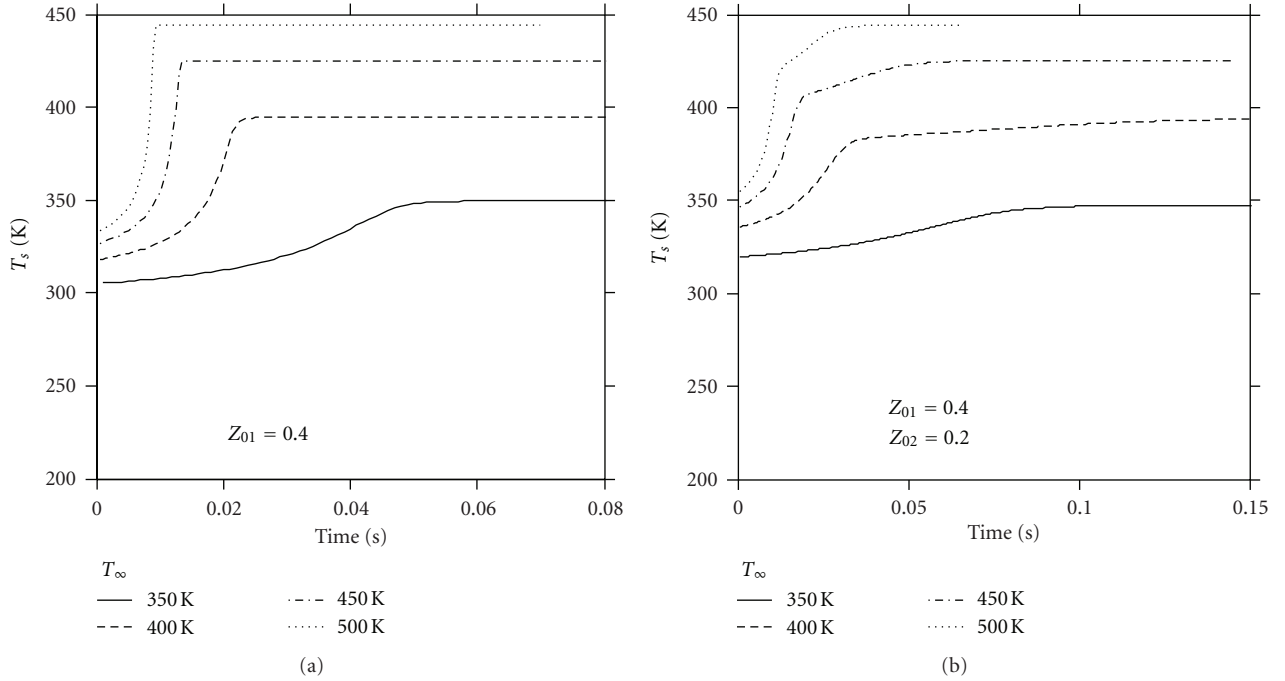


FIGURE 7: Temporal variation of equilibrium surface temperature at various ambient temperatures for a given initial composition of (a) binary mixture and (b) ternary mixture.

in Wilms [9]. The validated model is used to carry out parametric studies at atmospheric pressure under normal gravity, for a range of ambient temperatures. The parameters of interest such as the time histories of droplet surface area, liquid-phase composition, surface temperature, and the

evaporation constant have been predicted. The variation of time-averaged evaporation constant as a function of ambient temperature for different fuel compositions is also presented and discussed. For the binary mixture, comprised of n-heptane and n-hexadecane, the time-averaged evaporation

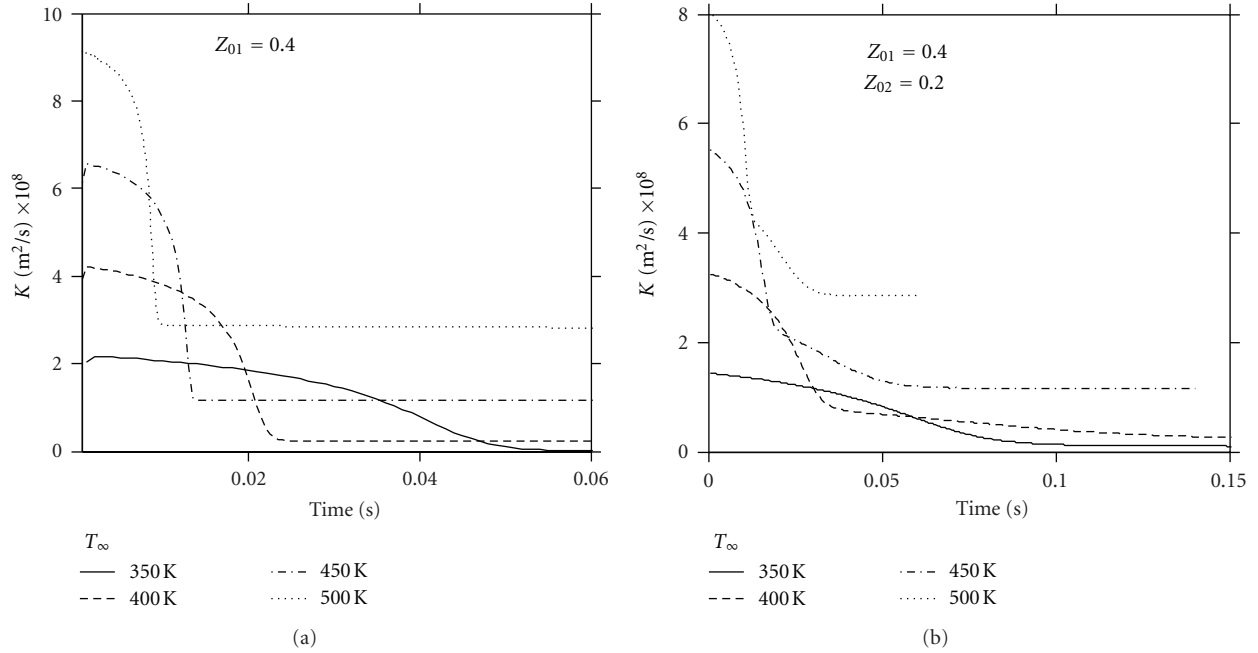


FIGURE 8: Temporal variation of the evaporation constant at different ambient temperatures for a given initial composition of (a) binary mixture and (b) ternary mixture.

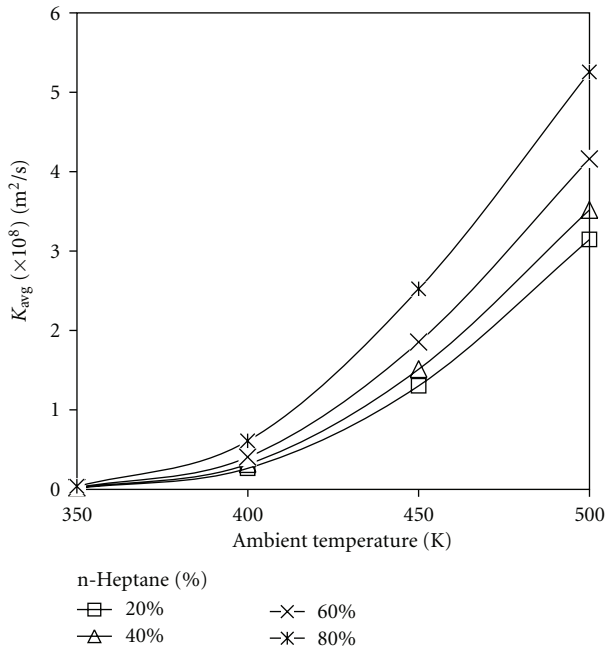


FIGURE 9: Variation of the time-averaged evaporation constant with ambient temperature for different initial compositions (volume %) of binary mixture.

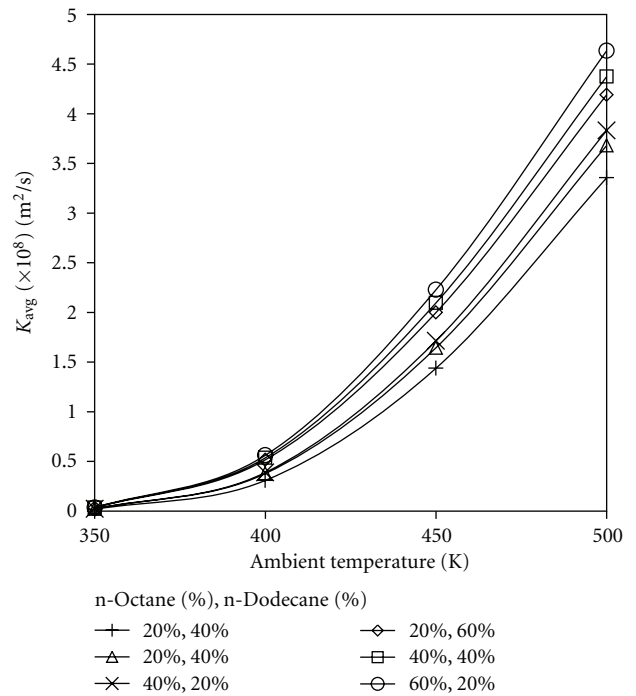


FIGURE 10: Variation of the time-averaged evaporation constant with ambient temperature for different initial compositions (volume %) of ternary mixture.

constant is seen to increase by around 225-times as the temperature is increased from 350 K to 500 K, for the composition having 80% n-heptane and 20% n-hexadecane. Similarly, when the ambient temperature is kept at 350 K,

and when the n-heptane volume percentage is increased from 20% to 80%, around 2.5-times increase in average evaporation value is observed. In the case of ternary droplets, for a blend composition of 20% n-octane, 20% n-dodecane,

and 80% n-hexadecane, when the ambient temperature is increased from 350 K to 500 K, around 195-times increase in the average evaporation constant is achieved.

References

- [1] A. Y. Tong and W. A. Sirignano, "Multicomponent droplet vaporization in a high temperature gas," *Combustion and Flame*, vol. 66, no. 3, pp. 221–235, 1986.
- [2] J. Tamim and W. L. H. Hallett, "A continuous thermodynamics model for multicomponent droplet vaporization," *Chemical Engineering Science*, vol. 50, no. 18, pp. 2933–2942, 1995.
- [3] S. Yang, Y. Ra, and R. D. Reitz, "A vaporization model for realistic multi-component fuels," in *Proceedings of the 22nd Annual Conference on Liquid Atomization and Spray Systems-USA*, pp. 16–19, Cincinnati, Ohio, USA, May 2010.
- [4] S. K. Aggarwal and H. C. Mongia, "Multicomponent and high-pressure effects on droplet vaporization," *Journal of Engineering for Gas Turbines and Power*, vol. 124, no. 2, pp. 248–255, 2002.
- [5] M. Rensizbulut and M. Bussmann, "Multicomponent droplet evaporation at intermediate Reynolds numbers," *International Journal of Heat and Mass Transfer*, vol. 36, no. 11, pp. 2827–2835, 1993.
- [6] Y. Ra and D. R. Reitz, "The application of a multicomponent droplet vaporization model to gasoline direct injection engines," *International Journal of Engine Research*, vol. 4, no. 3, pp. 193–218, 2003.
- [7] K. Gartung, S. Arndt, and C. Seibel, "Vaporization of multicomponent fuel droplets numerical and experimental evaluation," in *Proceedings of the 18th Annual Conference on Liquid Atomization and Spray Systems-Europe*, pp. 9–11, Zaragoza, Spain, September 2002.
- [8] G. Chen, S. K. Aggarwal, T. A. Jackson, and G. L. Switzer, "Experimental study of pure and multicomponent fuel droplet evaporation in a heated air flow," *Atomization and Sprays*, vol. 7, no. 3, pp. 317–337, 1997.
- [9] J. Wilms, *Evaporation of multicomponent droplets [Ph.D. thesis]*, Institute of Aerospace Thermodynamics (ITLR), University of Stuttgart, 2005.
- [10] S. R. Turns, *An Introduction to Combustion*, McGraw-Hill, New York, NY, USA, 2000.
- [11] K. Annamalai and I. K. Puri, *Combustion Science and Engineering*, CRC Press, New York, NY, USA, 2007.
- [12] R. C. Reid, J. M. Prausnitz, and J. P. O'Connell, *The Properties of Gases and Liquids*, McGraw-Hill, New York, NY, USA, 2001.
- [13] J. Gmehling, P. Rasmussen, and A. Fredenslund, "Vapor-liquid equilibria by UNIFAC group contribution. Revision and extension. 2," *Industrial and Engineering Chemistry Process Design and Development*, vol. 21, no. 1, pp. 118–127, 1982.

